Supplementary Information

A multistimuli responsive and self-healing zn (ii)-inosine supramolecular metal-organic gel: phase selective gelation and application as a light-responsive schottky barrier diode

Surbhi Singh,[a] Atul Kumar Sharma,[b] Kunal Rohilla,[a] Nisha Verma,[a] and Bhagwati Sharma*[a]

[a]*Materials Research Centre, Malaviya National Institute of Technology Jaipur, Malviya Nagar, Jaipur 302017, India.*

Email: bhagwati.mrc@mnit.ac.in

[b]*Department of Electronics and Communication Engineering, Malaviya National Institute of Technology Jaipur, Malviya Nagar, Jaipur 302017, India.*

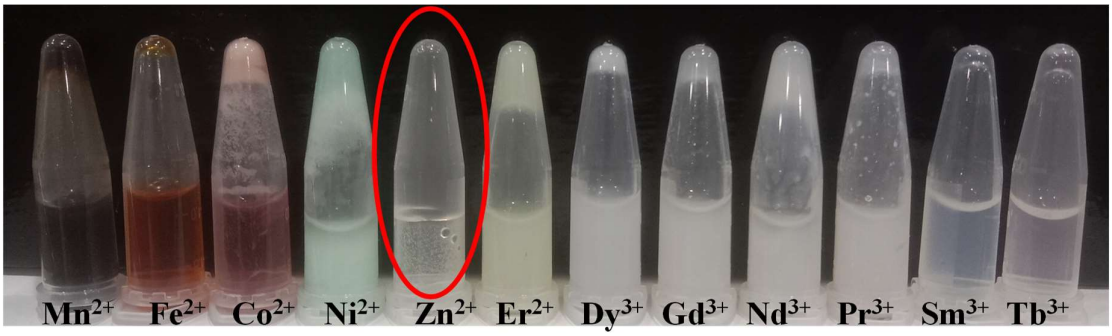

Figure S1. Digital images showing the specificity of Zn^{2+} ions towards the formation of hydrogel upon interaction with inosine.

Figure S2. Digital image of Zn-I metallogel after 6 months, showing the stability of the gel.

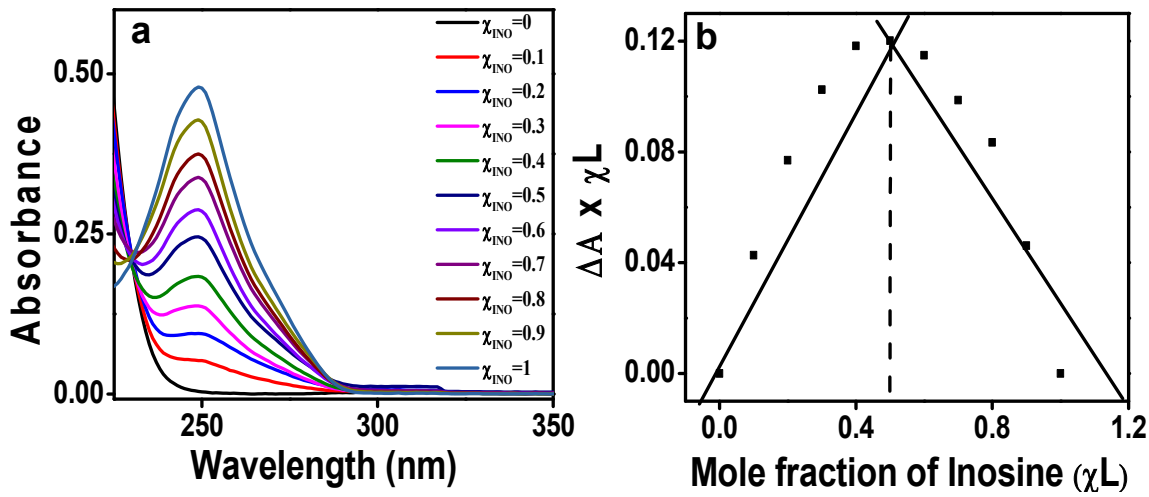

Figure S3. (a) Changes in the UV-visible spectra of $Zn(CH_3COO)_2$ (5 x 10^{-5} M) upon addition of different mole fractions of inosine (5 x 10^{-5} M) (b) Job's plot obtained by following the absorbance at 250 nm, indicating a 1:1 metal-ligand stoichiometry.

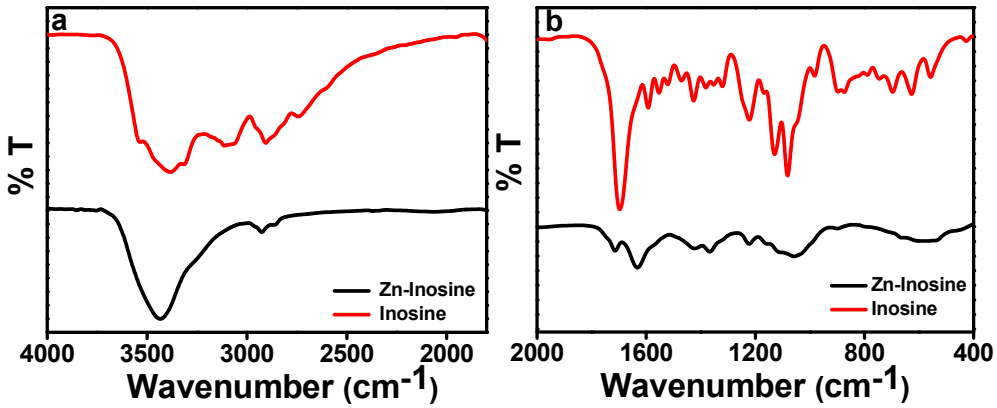

Figure S4. FTIR spectrum of inosine and Zn-inosine xerogel in the region (a) 4000-2000 cm^{-1} and (b) 2000-400 cm^{-1}.

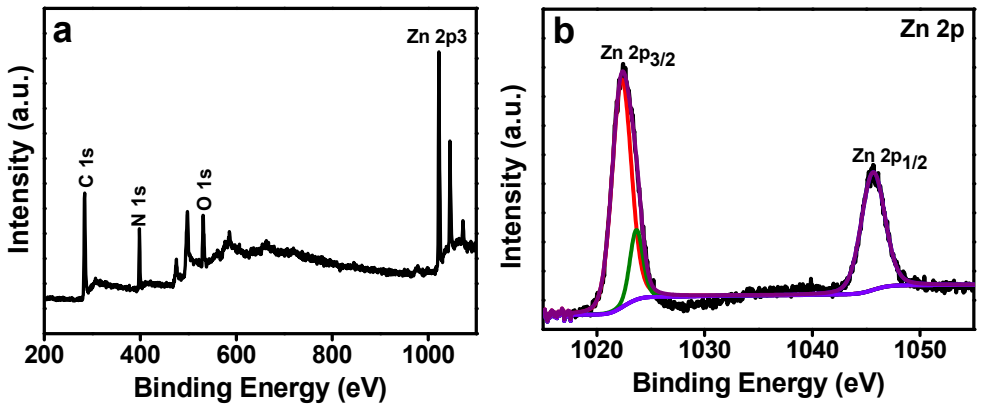

Figure S5. XPS spectra of Zn-inosine metallogel: (a) Survey spectrum and (b) Zn2p spectrum

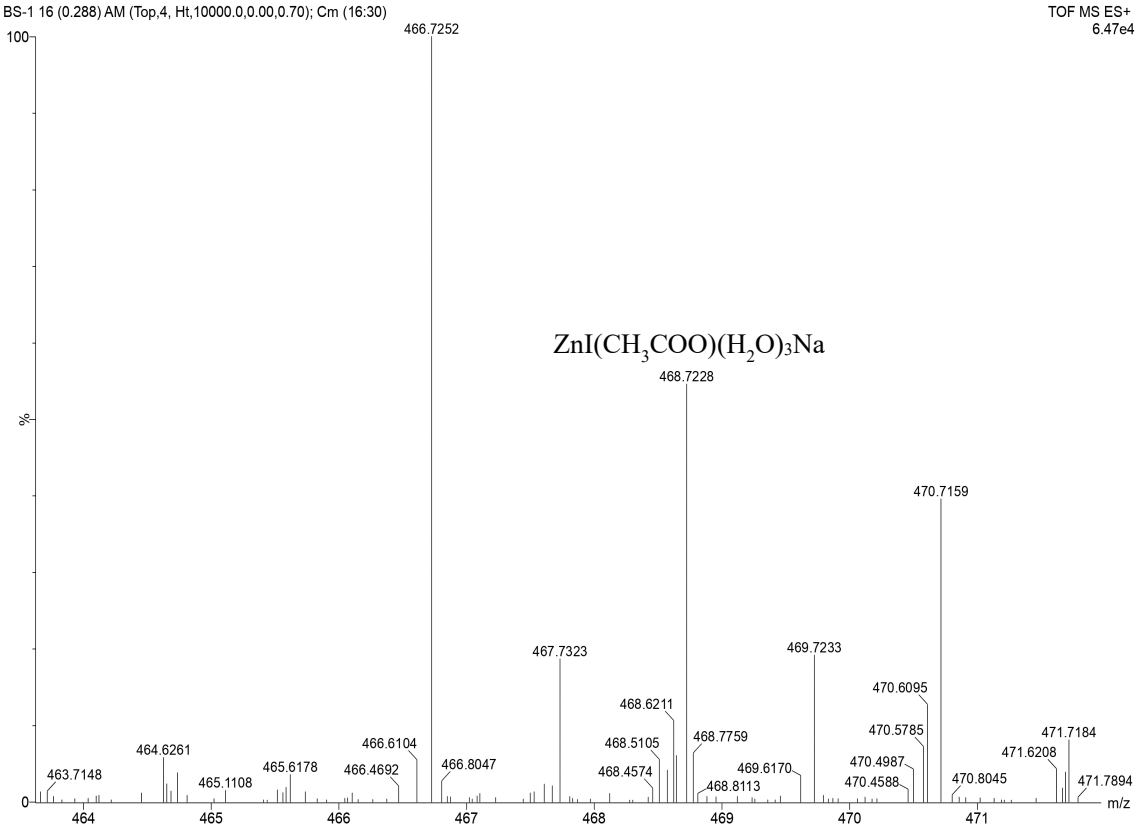

Figure S6. ESI- MS spectrum of a 1:1 mixture of inosine and zn-acetate (both 20 mM).

Figure S7. Digital image showing the formation of viscous sol at 20 mM concentration of both the precursors.

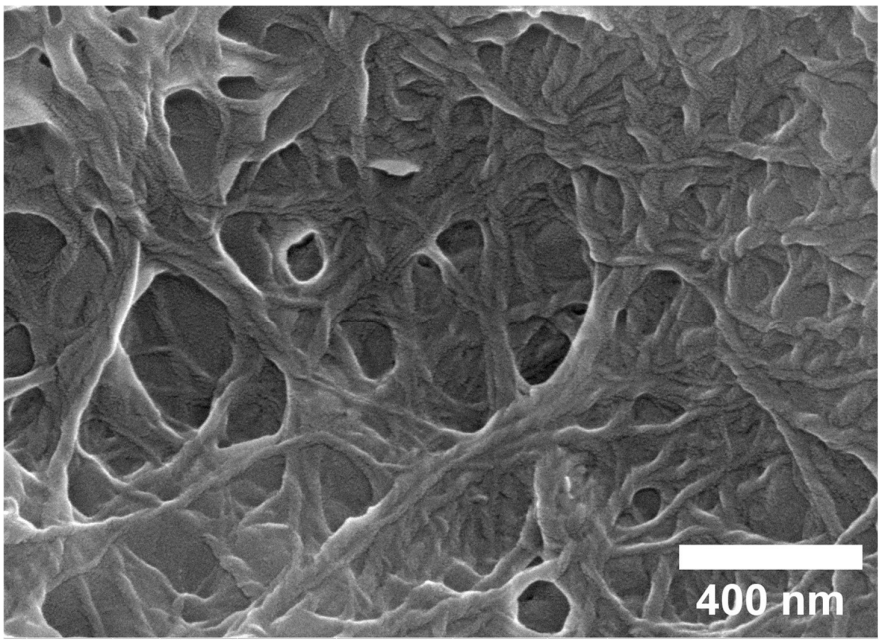

Figure S8. FESEM image of the viscous sol at a concentration of 20 mM for both the precursors showing nanofibrous morphology.

Table S1. Interaction of Inosine with Zn^{2+} ions with varying molar ratios (With a variation in the molar concentration of both the reactants).

Inosine (M)	Zinc Acetate (M)	Result
0.05	0.1	Weak Gel
0.075	0.1	Gel
0.1	0.1	Strong Gel
0.1	0.075	Gel
0.1	0.05	Weak Gel

Figure S9. (a) Digital image of a 1:1 mixture of Inosine (dissolved in 1M HCl) and Zn-acetate, showing the formation of a clear solution.

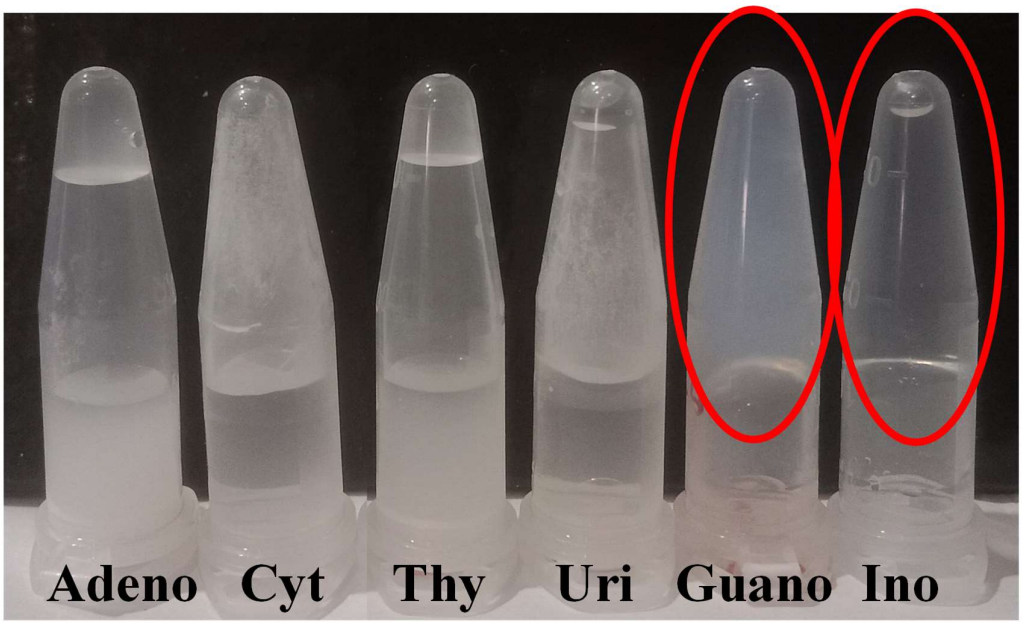

Figure S10. Digital images showing the specificity of guanosine and inosine among different nucleosides towards the formation of hydrogel upon interaction with Zn^{2+}.

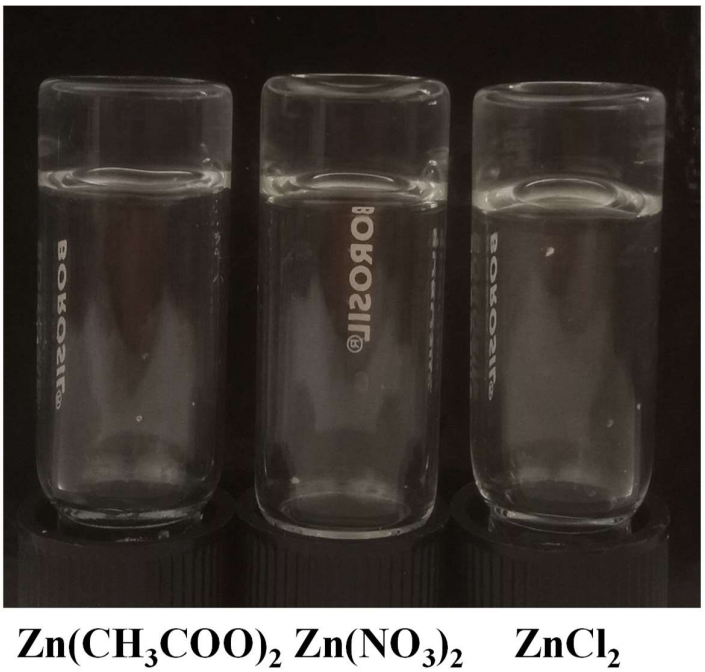

Figure S11. Digital images showing the formation of stable gels upon changing of metal counterions viz. $Zn(CH_3COO)_2$, $Zn(NO_3)_2$ and $ZnCl_2$ respectively.

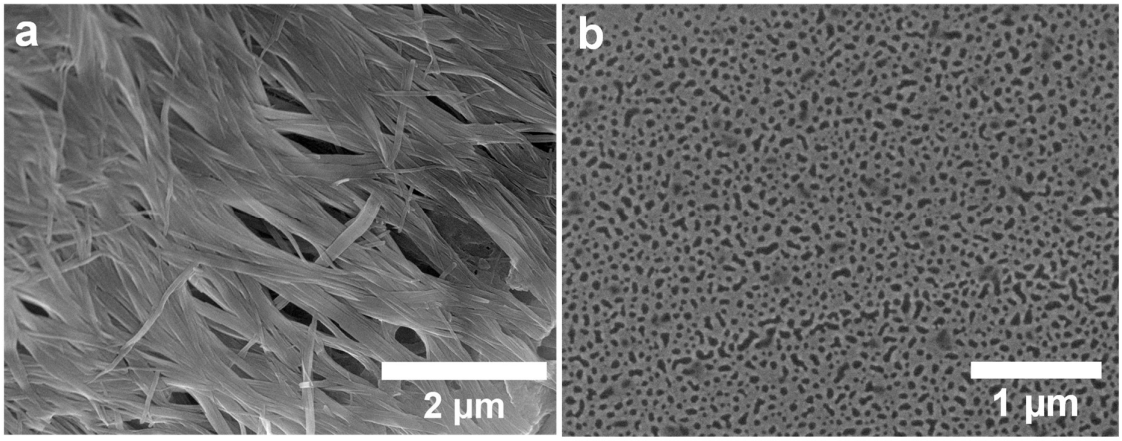

Figure S12. FESEM image showing the formation of fibers upon changing of metal counterion to (a) Zinc Nitrate and (b) Zinc Chloride.

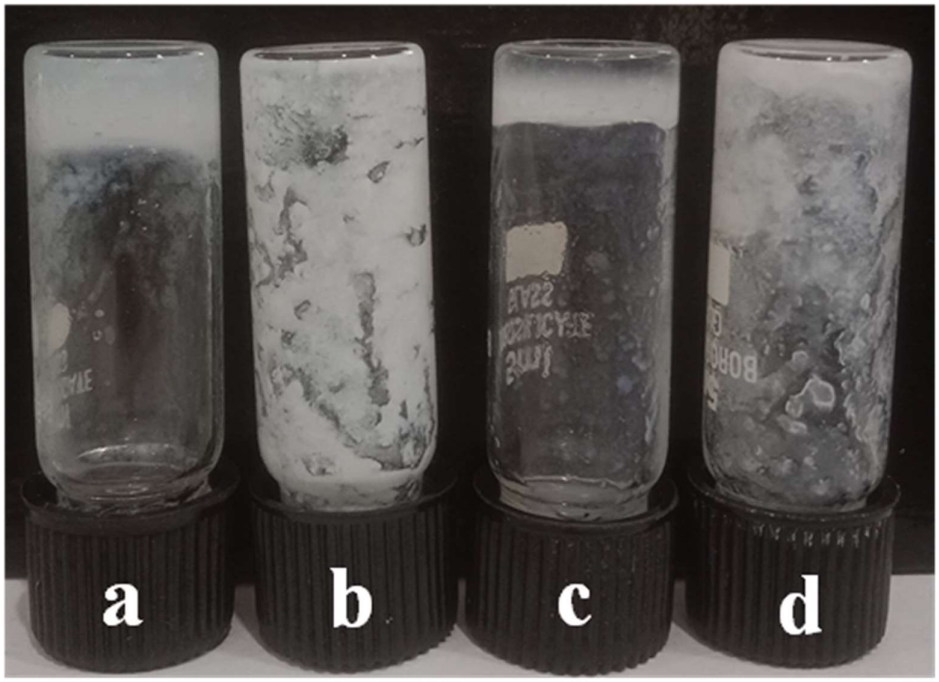

Figure S13. Digital images of Zn-Inosine mixtures in different solvents (a) methanol-water (gel) (b) methanol-methanol (precipitate) (c) ethanol-water (gel) and (d) ethanol-ethanol (precipitate) respectively.

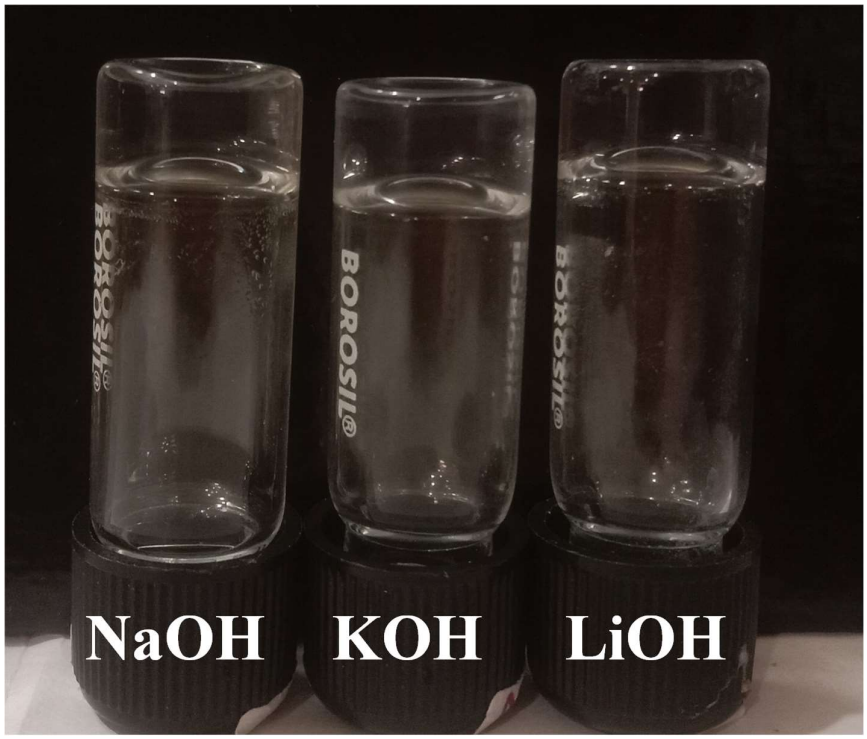

Figure S14. Digital images showing the formation of stable gels upon changing bases viz. NaOH, KOH and LiOH respectively, implying that gel formation is not specific to any particular base.

Figure S15. Digital images showing the interaction of zinc ions with inosine at different pH (from 7 to 13.3).

Table S2. pH measurement of inosine solution after addition of varying concentrations of NaOH and fixed volume of 0.1 M $Zn(CH_3COO)_2.2H_2O$.

Sample ID	Quantity of Inosine (mg)	Volume of water taken (mL)	Volume of added NaOH (1M) (mL)	Measured pH	Volume of $Zn(CH_3COO)_2$ (0.1M) added (mL)	Final pH after addition of $Zn(CH_3COO)_2$	Result
L1	134	4.0	1.0	12.55	5	7.0	Transparent Gel
L2	134	3.5	1.5	13.0	5	10.1	Turbid Gel

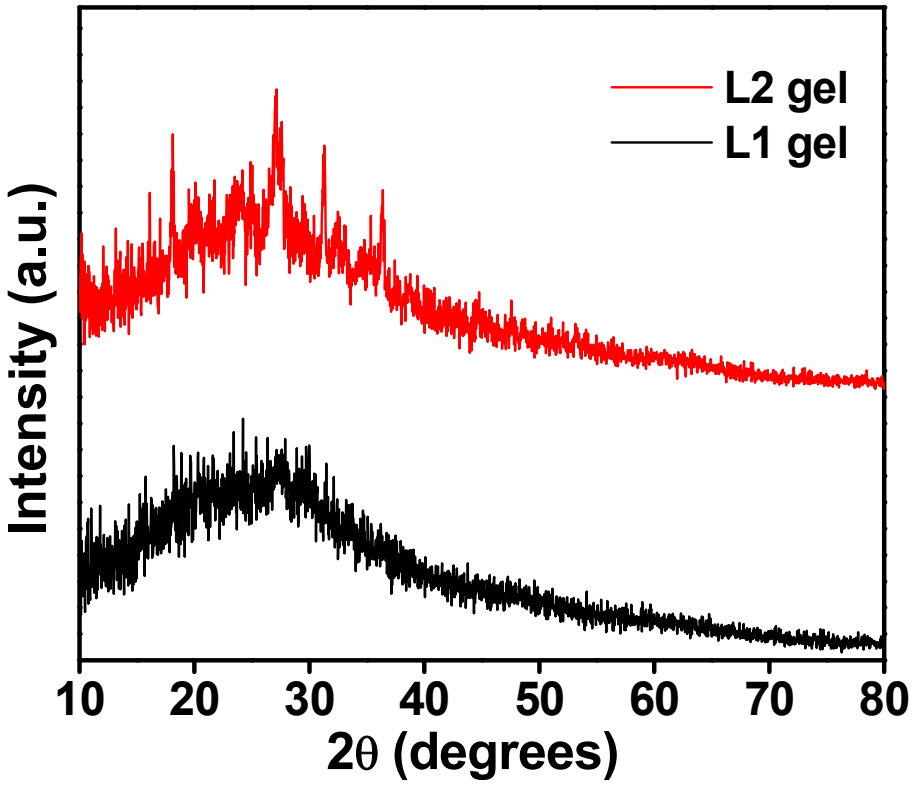

Figure S16. PXRD pattern of freeze dried xerogel prepared using inosine solution with a pH of 12.5 (L1) showing an amorphous nature of the gel and inosine with a pH of 13.0 (L2) showing some crystalline peaks.

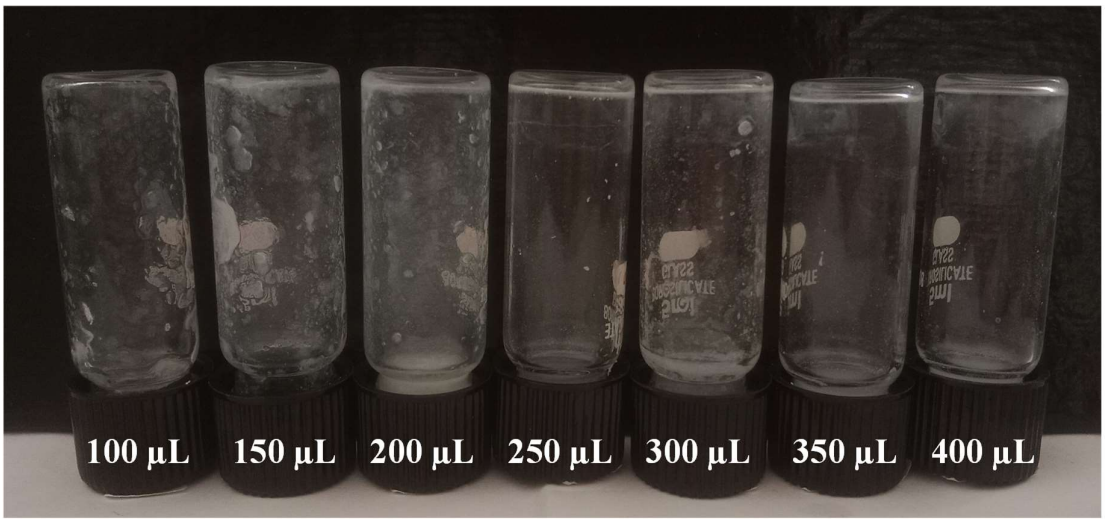

Figure S17. Digital images showing the interaction of Zn^{2+} ions using different concentrations of NaOH without the use of inosine leading to the formation of turbid sol.

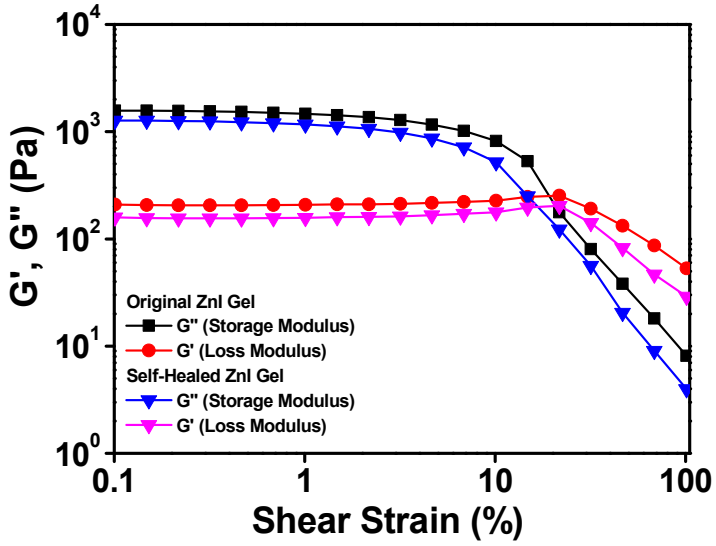

Figure S18. (a) Dynamic strain sweep rheological investigation of the original and self-healed Zn-inosine gel.

Figure S19. Digital images showing the stability of zn-inosine metallogel at different NaOH Concentrations from 100 µL/ ml to 300 µL/ ml.

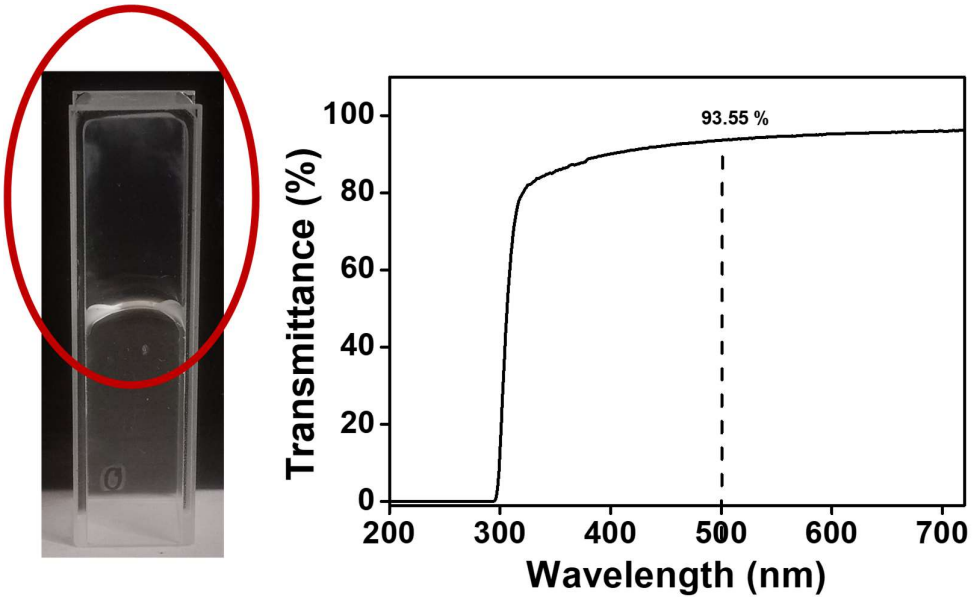

Figure S20. Digital image and transmittance spectra of transparent Zn:Inosine metallogel.

Optical Characterization

The optical band gap of the Zn-I xerogel was estimated using the well-known Tauc's equation given in equation S1

$$(\boldsymbol{\alpha h\nu}) = \boldsymbol{A}(\boldsymbol{h\nu} - \boldsymbol{E_g})^{\boldsymbol{n}} \quad \text{(S1)}$$

where the usual notation for *α, Eg, h,* and *v* is given. Two constants appear in this equation: *"n"* which is dependent on the electron transition, and *"A"* which, in the best-case scenario, has a value of 1. For our synthesized metallogel, the calculated direct band gap (Optical) (Eg) is 3.8 eV.

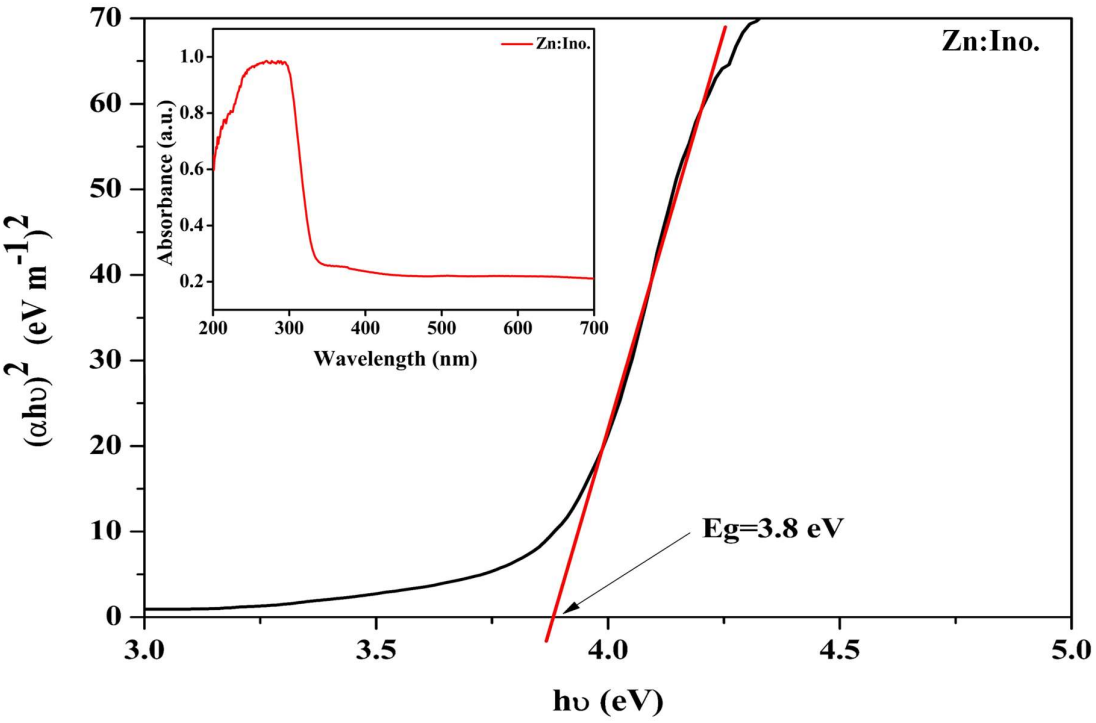

Figure S21. UV−vis absorption spectra (inset) and Tuac's plots for Zinc-Inosine metallogel.

Device Fabrication and Parameters

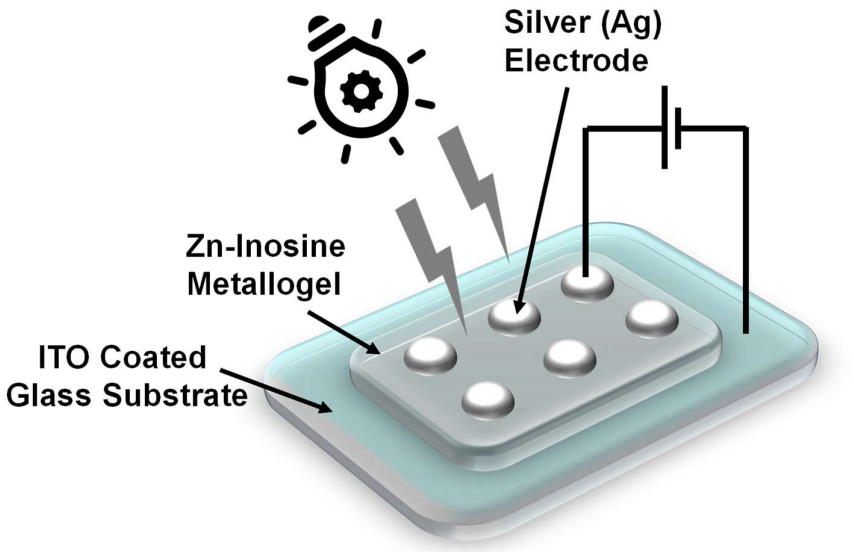

Scheme S1. A schematic representation of Schottky diode fabrication using Zn-Inosine metallogel.

Thermionic emission theory has been used to evaluate the $I-V$ characteristic of the synthesized metallogel based Schottky barrier diode (SBD). Important diode parameters have also been extracted using Cheung's approach. In this sense, the acquired I-V curve has been subjected to a quantitative analysis using the standard equations shown below:

$$\boldsymbol{I = I_0 exp\left(\frac{qV}{\eta KT}\right)\left[1 - exp\left(\frac{-qV}{\eta KT}\right)\right]} \quad \text{(S2)}$$

$$\boldsymbol{I_0 = AA^{*}T^{2} exp\left(\frac{-q\emptyset_B}{KT}\right)} \quad \text{(S3)}$$

where I_0, electronic charge, temperature in Kelvin, Boltzmann constant, forward bias voltage, effective diode area, ideality factor, and effective Richardson constant are, respectively, represented by the symbols k, T, V, A, η and A^*. For the fabricated device an effective Richardson constant of 32 AK^{-2} cm^{-2} was considered.

Equations S4 to S6, which were taken from Cheung's method, were also used to calculate the series resistance, ideality factor, and barrier potential height.

$$\frac{dV}{d(lnI)} = \left(\frac{\eta KT}{q}\right) + IR_S \tag{S4}$$

$$H(I) = V - \left(\frac{\eta KT}{q}\right) ln\left(\frac{I}{AA^*T^2}\right) \tag{S5}$$

$$H(I) = IR_S + \eta \emptyset_B \tag{S6}$$